A transferrin receptor-binding mucoadhesive elastin-like recombinamer: *in vitro* and *in vivo* characterization

Constancio Gonzalez-Obeso[1], Alessandra Girotti[1], J. Carlos Rodriguez-Cabello[1,*]

[1] BIOFORGE (Group for Advanced Materials and Nanobiotechnology), CIBER-BBN, University of Valladolid, Spain, Paseo de Belén 19, 47011.

[*]roca@bioforge.uva.es, Fax: +34 983184698

1. Abstract

The development of mucoadhesive materials is of great interest and is also a major challenge. Being adsorption sites, *mucosae* are suitable targets for drug delivery, but as defensive barriers they are complex biological surfaces to interact with, mainly due to their protective mucus layer. As such, first- and second-generation mucoadhesives focused on material-mucus interactions, whereas the third generation of mucoadhesives introduced structural motifs that are able to interact with the cells beneath the mucus layer. The combination of different prerequisites (water solubility, soft gel formation at body temperature and able to interact with the mucus) in a single molecule is easily achieved using elastin-like recombinamers (ELRs) given their multiple block design. Moreover, we have been able to introduce a short amino-acid sequence known as T7 that is able to bind to transferrin receptors in the epithelial cell layer. The T7 sequence enhances the cell-binding properties of the mucoadhesive ELR (MELR), as demonstrated using a Caco-2 epithelial cell model. *In vivo* experiments confirmed the mucoadhesive properties found *in vitro*.

Keywords: *Transferrin receptor, T7 peptide, elastin-like, mucoadhesion, Caco-2.*

2. Introduction

Since the first report concerning the use of a mucoadhesive [1], the development of bioadhesive polymers for use as drug-delivery systems has received significant attention [2, 3], due to the

intrinsic properties of bioadhesive devices, namely: localization of the dosage form in adsorption tissues, close contact with the absorbing surface avoiding leakage of the drug, and, an extended residence time, which allows a more continuous and homogeneous dosage, thereby improving patient compliance [4].

Mucoadhesion is a specific type of bioadhesion in which at least one of the surfaces is a mucosa [5]. Mucosa is a multilayered tissue that covers the outer surface of organs that are in contact with the exterior. It plays a very important homeostatic role as it serves as both a door for the uptake of substances of interest and as a defense barrier against undesired substances and microorganisms [6]. To facilitate this defense/barrier function, goblet cells secrete mucus on the apical side of the epithelium forming a continuous protective layer. Mucus is a natural hydrogel mainly comprising water, salts, lipids, defense proteins and mucin [7], being the latter responsible for the viscous, gel-like behavior of mucus [8].

First-generation mucoadhesives focused on their ability to interact and adhere to mucus. Mucoadhesion is a very complex process that is yet to be fully understood [9]. Several theories have been elaborated in order to explain why a material is mucoadhesive or not [10], but none of these theories alone can explain the complete mechanism as to why a material is mucoadhesive. Instead, mucoadhesion is described as a set of different stages, each of them characterized using different techniques [11-15]. A second generation of mucoadhesives, still exclusively focused on the interaction of the material with mucus, was produced by enriching materials with mucus-interacting moieties, such as cysteines [16, 17], or bacteria-derived moieties [18].

The third generation of mucoadhesives extended the ability of the mucoadhesive to interact with the underlying cell layer in addition to the mucus layer, thereby extending the residence time [19]. Such interactions can be specific [20] or non-specific, such as bacterial [21] and non-immunogenic plant-derived lectins [22, 23]. Their major drawback is their non-specifically binding to other carbohydrates present in the mucus, thereby decreasing their efficiency. Another important issue to be assessed is the fact that, besides the flushing effect of food/drink and the inherent dilution effect of the mucoadhesion process (the mucoadhesive dilutes as it defuses into

the mucus), the physical properties that allow a material being mucoadhesive should be maintained [24, 25].

The transmembrane transferrin-receptor (TfR) is a potential luminal target as it is present throughout the gastrointestinal tract [26-30]. The T7 peptide, a seven amino-acid sequence peptide that has been proven to efficiently and selectively bind to the TfR [31-33] but does not interfere the endocytosis pathway itself [34], is one of them. Physiologically relevant intestinal epithelial cell models are needed in order to characterize cell-material interactions. Of the various intestinal endothelial models, human adenocarcinoma Caco-2 cells are particularly suitable [35] as, when cultured under specific and well-established conditions [36], they spontaneously differentiate, expressing several morphological and biochemical characteristics of small intestinal enterocytes [37], including the TfR [38]. The last stage in the characterization of a mucoadhesive material is its performance in the most realistic and adverse environment, namely *in vivo*, where rats are frequently used as the *in vivo* model for mucoadhesive tests [39, 40]. Enteral administration offers many advantages as it permits a time- and dose-controlled administration of non-sterile substances.

Recombinant proteinaceous materials have on-demand properties, easily tailored by their amino acid composition. Among them, elastin-like recombinamers (ELRs) are suitable candidates for the development of new applications. ELRs sequence is inspired by the elastomeric domains of natural tropoelastin, and is based on the repetition of the pentapeptide (VPGXG), where X is the guest amino acid residue and can be any natural amino acid except proline. This pentapeptide exhibits an inverse temperature transition (ITT) characterized by a transition temperature (T_t) above which these pentapeptides become water-insoluble [41]. Their block design and recombinant origin allows us to tailor their amino-acid sequence, charge, molecular weight and structure, thus providing a single molecule with a combination of highly specific properties required to achieve the desired goal [42], which are not found, simultaneously, in other materials. Moreover, their proteinaceous origin permits their elimination via natural degradation pathways without generating harmful side products. The correct combination of blocks leads to

thermoresponsive hydrogel-forming ELR, which permits their application in liquid state, facilitating the intimate contact with the surface to adhere, while their hydrogel-forming capacity provides increased mechanical properties.

In this work, we have rationally designed, developed, produced and characterized what, to the best of our knowledge, is the first thermoresponsive hydrogel-forming ELR with mucoadhesive properties. The ELR-mucus interaction has been extensively characterized *in vitro*, and Caco-2 cell model has been used to investigate the interaction between the T7-MELR and the intestinal epithelial layer [43]. Thus, its enhanced cell-interaction properties via the TfR-binding sequence, as well as the absence of cytotoxicity were assessed *in vitro*; while the mucoadhesive properties of the designed ELR were assessed *in vitro* and confirmed *in vivo* in a rat model.

3. Materials and Methods

3.1. ELR biosynthesis, purification and characterization

The ELRs used in this work were obtained using genetic-engineering techniques and *Escherichia coli* biosynthesis, as described previously [44]. All restriction and modification enzymes were purchased from Fermentas. The T7 encoding sequence was synthetized by NZYTECH (Portugal) and incorporated into the ELR sequence at the C' terminus using the same genetic-engineering techniques. The correctness of the ELR gene sequences was corroborated by gene sequencing (external service, Cenyt Support System). Hereinafter the ELR lacking the T7 sequence will be referred to as MELR (mucoadhesive ELR) and the T7-tagged MELR as T7-MELR.

3.2. Turbidimetry

Turbidity measurements were performed at a wavelength of 650 nm and a temperature of 37°C in ultrapure water using a Varian Cary 50 UV-Visible Spectrophotometer, equipped with a single cell Peltier device to control the temperature, as described previously [45].

For all three particle methods (turbidimetry, Z-potential and size distribution) a 2 mg/mL mucin suspension in ultrapure water was prepared as described in section 3.2. The average mucin

concentration of the supernatant was evaluated by freeze-drying known volumes of suspension (at least 8 samples from different preparations), giving an average mucin concentration of 1.71±0.09 mg/mL. An equal volume of different concentrated T7-MELR solutions ranging from 0.5 to 7 mg/mL ELR was added to this mucin suspension. Thus, the mucin suspension was kept constant at 0.85 mg/mL while the ELR concentration ranged from 0.25 to 3.5 mg/mL.

3.3. Size and Z-Potential

Dynamic light scattering (DLS) measurements (size and Z-potential) were performed using a Zetasizer nano ZSP (Malvern Instruments) equipped with a 10mW He−Ne laser at a wavelength of 633 nm at 37°C. Samples were prepared as described for turbidity measurements.

Each experimental point was evaluated in three independent experiments, performing four measurements each time. The values presented are the average of these measurements and the error is the standard deviation (SD).

3.4. Differential scanning calorimetry (DSC)

DSC experiments were performed in a METTLER TOLEDO DSC 822 with liquid nitrogen cooler. The temperature ramp was set from 0 to 80°C at 5°C/min with an initial isothermal stage at 0°C for 5 min. For T7-MELR measurements, 20 µL of a 100 mg/mL solution was used, while for mucin 20 µL of a 113 mg/mL solution was used, both in ultrapure water. Ultrapure water was used as the reference. To assess the possible influence of mucin on the thermal properties of the T7-MELR, 20 µL of a mixture of equal volumes of a 200 mg/mL solution of T7-MELR and a 226 mg/mL mucin suspension, both in ultrapure water, was analyzed. A 113 mg/mL mucin solution was used as reference.

3.5. Rheological measurements and mechanical properties

Rheological measurements were performed using a TA Instruments AR2000ex rheometer equipped with a Peltier plate for controlling the temperature, using a 40 mm flat geometry, 1 Hz and 0.2% strain and depositing 600 µL of the sample. Temperature ramps were performed from 5 to 37°C, at 4°C/min.

T7-MELR and mucin were dissolved at 100 and 113 mg/mL, respectively, in ultrapure water. The T7-MELR plus mucin mixture was prepared by dissolving and mixing equal volumes of 200 and 226 mg/mL solutions of T7-MELR and mucin, respectively. A time course for determining evolution of the mechanical properties of T7-MELR was performed. Thus, 100 mg/mL solutions of T7-MELR in ultrapure water were incubated at 37°C under hermetic conditions and the mechanical properties of the samples were measured after 3, 5, 7, 9 and 12 days at 37°C. The G' and G'' values presented for each time point are the mean of three different samples.

3.6. Tensile measurements

Tensile measurements were performed using an Instrong Universal Testing Machine (MOD. 5.500R6025) equipped with a 0.5-50 N load head. For ELR and mucin samples, filter paper was wetted with a 100 mg/mL solution of T7-MELR at 4°C or 113 mg/mL mucin in ultrapure water and allowed to dry at 37°C. For tensile tests, a double-sided adhesive tape was used to keep samples (3x3 cm) attached to the test plates.

Samples were hydrated with 200 µL of ultrapure water for 1 minute at room temperature, then compressed (0.2 mm/min) up to 5 N of load [46], maintained during 2 minutes. The sample was then detached at a constant speed of 0.01 mm/s [46, 47] while force and distance were recorded. The values presented are the mean of at least five measurements and the error is the SD.

3.7. Cell culture

Human epithelial colorectal adenocarcinoma cells (Caco-2) were purchased from ATCC (ATCC® HTB-37), and basal medium, high glucose Dulbecco's modified Eagle's medium (DMEM), fetal bovine serum (FBS), non-essential amino acids (NEAA), penicillin streptomycin solution, trypsin-EDTA (Corning, Ref. 25-052-CV), phosphate-buffered saline (PBS) and Dulbecco's phosphate-buffered saline (DPBS), Trypan Blue stain 0.4%, Alexa Fluor 488 phalloidin, LIVE/DEAD® Viability/Cytotoxicity Kit, for mammalian cells, Alamar Blue® and DAPI stain were supplied by Invitrogen. Holo-transferrin (HTf) was purchased from Sigma (Ref. T0665). All cell culture plastic-ware and consumables were purchased from NUNC, except

inserts and 24-well plates (Transwell Permeable Supports, 6.5 mm Insert, 24-well plate, 0.4 µm pore size polyester membrane, REF: 3470), which were purchased from Costar.

Caco-2 cells were cultured in DMEM supplemented with 10% FBS, penicillin (100 U/mL), streptomycin (100 µg/mL) and 1% NEAA. The medium was replaced every two days and maintained at 37 °C in a 5% CO_2 humidified environmental chamber. Cells were harvested with Trypsin-EDTA enzymatic treatment at 80% confluence and cell counts were evaluated using a standard Trypan Blue exclusion assay. Caco-2 cells passage 43-45 were utilized in all cell-culture experiments.

3.7.1. Cell-binding assays

Intestinal epithelial interaction tests were carried out over differentiated Caco-2 cell monolayers. Cell differentiation was carried out following the protocol described by Hubatasch *et al*. [36]. The integrity of the cell monolayer was assessed by actin staining with phalloidin [48] (See Supporting Information). Binding assays were performed as follows: after cell differentiation, cells were co-incubated with FITC-modified MELR and T7-MELR (See Supporting Information) dissolved in complete medium at 1 or 5 mg/mL for 30 or 120 minutes. The medium was then removed and the samples washed three times with DPBS at 37°C. The adhered MELR or T7-MELR were quantified using a microtiter plate reader by measuring the fluorescence associated with the FITC (Ex. 490 nm, Em. 525 nm, Cutoff 515 nm).

3.7.2. Competitive binding assays

To determine non-specific binding, human HTf was used as T7-MELR competitor for TfR binding. Briefly, after Caco-2 differentiation, cells were incubated with HTf (2 mg/mL, 25 µM) dissolved in complete medium for 120 minutes, then the medium was removed and FITC-modified T7-MELR and MELR (5 mg/mL, 43µM) with 2 mg/mL of HTf solution was incubated for 120 min. Cells treated only with HTf and untreated cells were used as controls. Subsequently, samples were washed three times with DPBS at 37°C in order to remove unbound ELR. T7-MELR and MELR quantification was performed using a microtiter plate reader. Three

independent experiments were performed with at least three repetitions for each experimental point.

3.8. Statistical analysis

The influence of ELRs on cell viability and the interaction efficacy with mucin, as well as *in vitro* experimental results, were analyzed using a Student's t-test analysis of variance for paired samples, with a significance level (α) of 0.05. All treatment-related effects and measurements were considered to be statistically significant if p was less than 0.05. All data were analyzed using Sigma Plot 12 (Systat Software Inc.). *: p value of 0.05; **: p value of 0.01; ***: p value of 0.001.

3.9. *In vivo* experiments

The *in vivo* experimental protocol was approved by the University of Valladolid Ethics Committee. The experiment was conducted in accordance with national guidelines for animal care, as set out in RD 1201/2005, on the protection of animals used for experimental and other scientific purposes, which transposes and implements European Directive 86/609/CEE. For the *in vivo* assay, rats (*Rattus norvegicus*) weighing 250-300 g were provided by the University of Valladolid animal facility.

A steel, round-ended gavage (Hardvardapparatus, ST2 34-0317 Dosing Cannula, 75 mm, 16 G, Straight) coupled to a 1 mL syringe was used for enteral administration of 300 µL of a 100 mg/mL solution of FITC-modified T7-MELR in PBS to rats fed *ad libitum*. The animals were then randomly distributed into three groups, and sacrificed at 3, 5 and 7 hours post-administration. As a negative control, 300 µL of PBS was administered to 3 rats, which were euthanized after 3 hours. Rats were euthanized with CO_2 and their gastrointestinal tract was extracted and divided into seven different sections: stomach, small intestine (subdivided into 4 equal segments), gut and large intestine. Each section was opened and the contents extracted and weighed. Samples, with their luminal side exposed, were incubated in 5 mL PBS under orbital agitation overnight at 4°C in order to dissociate the attached FITC-T7-MELR. The fluorescence of the washing solution was then measured using a microplate reader (SpectraMax M2e Multimode Microplate Reader, with

SoftMax Software, Molecular Devices; excitation wavelength: 490 nm; emission wavelength: 525 nm).

4. Results and discussion

4.1. ELR design and synthesis

The ELRs were designed with two main features in mind: first, an ability to self-gel in response to a temperature increase, and second, an ability to interact with the mucous layer covering the gastrointestinal mucosa. Moreover, a more complex MELR including a tagged TfR-binding sequence designed to interact with the epithelial cell layer beneath the mucus (T7-MELR; Figure 1) was constructed. Each feature is related to different functional regions, all of which can be included in a single molecule thanks to the genetically engineered origin of the MELRs. The thermoresponsive hydrogel-forming region itself comprises three smaller blocks: 2 of which form an physical hydrogel at body temperature (E50I60) [49]; and a third block named SILK, which stands for the amino acid sequence $(GAGAGS)_{10}$, is included in order to stabilize the hydrogel formed via the formation of β-sheets [50]. The mucin interacting region, $(VPGKG)_{144}$, includes a lysine as the guest amino acid, which confers properties that are essential for its intended use: first, its high T_t [51, 52], ensures that this block is completely water-soluble and remains in an extended and flexible conformation [53], which is essential for the ELR-mucin interaction to occur [54]; second, its high molecular weight is beneficial for the physical entanglement with mucin chains [55, 56]; and third, lysines are positively charged at pH≤10.5, which permits an electrostatic interaction with the negatively charged mucin [14, 57]. A TfR-binding sequence has been included at the C' terminus, flanking this mucin interacting region, via a flexible glycine linker (GGGGGG-HAIYPRH; T7). Purity, correctness of the sequence, molecular weight and thermal properties were extensively characterized. The overall results showed a high purity and appropriate composition for both materials (See Supporting information).

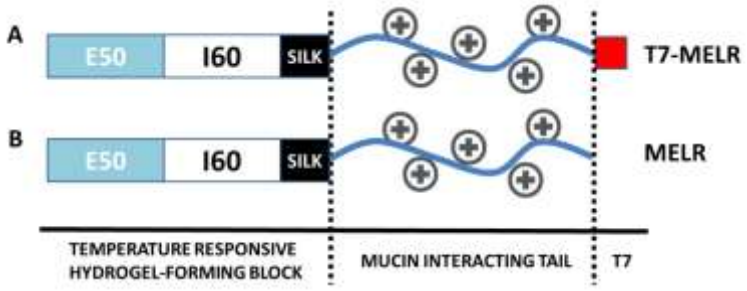

Figure 1. Schematic representation of (A) the T7-MELR and (B) the MELR. The different functional regions are highlighted.

4.2. Thermoresponsiveness of the T7-MELR

DSC is a suitable technique to characterize the thermosresponsiveness of ELRs, providing values for the T_t and latent heat of transition [58]. The T_t of the T7-MELR in ultrapure water at pH 7.3 was found to be 19.3 °C, with a latent heat transition of -5.62 $J \cdot g^{-1}$ (Figure 2). These findings are consistent with previous studies [51] of ELRs in which the thermoresponsive block bears isoleucine as the guest amino acid. Further studies of the thermal properties of the MELR and T7-MELR at different pH values can be found in the supporting information (SFigure8).

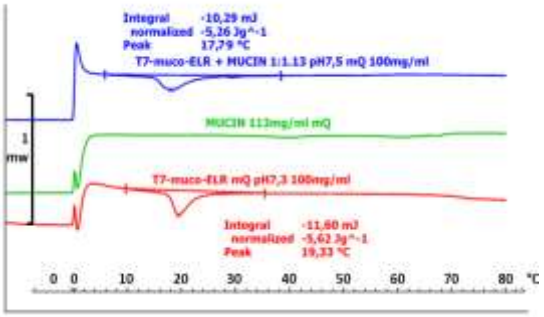

Figure 2. Transition temperature obtained by DSC measurements of T7-MELR alone at 100 mg/mL (red), mucin at 113 mg/mL (green) and T7-MELR plus mucin in a 1:1.13 ratio, with 100 mg/mL of the ELR (blue).

4.3. T7-MELR gel formation

The ability to form hydrogels in response to temperature ensures an increased mechanical stability of the material when placed inside the human body. As can be seen from Figure 3A, an increase in the temperature of T7-MELR solution leads to the formation of a hydrogel with an elastic modulus of 215 Pa and a loss modulus of 45.3 Pa. These mechanical properties arise from the

physical crosslinking of the thermoresponsive block [49], although it is a transient gel state and the mechanical properties decrease drastically with time [59]. Subsequently, the silk motifs start to physically crosslink via the formation of β-sheets. In order to assess the effect of the silk motifs, a time course was performed to determine the evolution of the mechanical properties of T7-MELR. As can be seen in Figure 3C, the gel state, which has very low elastic and loss moduli, is recovered after incubation for 3 days at 37°C. As the incubation time is extended, both the elastic and loss moduli increase, reaching a plateau value of 98.8 Pa for the elastic modulus and 25.8 Pa for the loss modulus after incubation for 12 days.

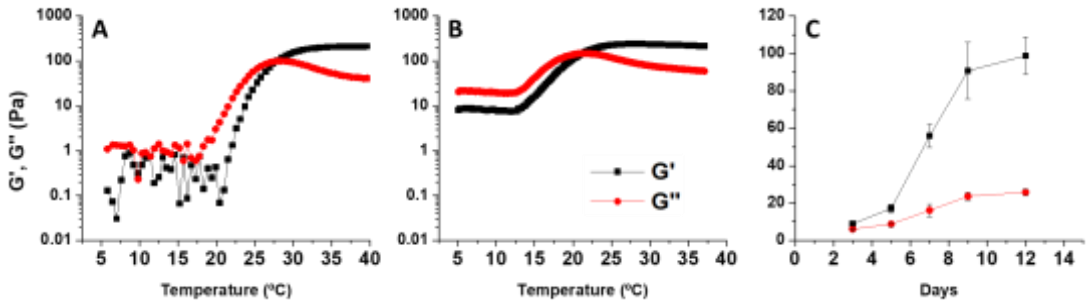

Figure 3. Gelation in response to temperature of (A) T7-MELR alone at 100 mg/mL in ultrapure water and (B) T7-MELR and mucin mixture at an ELR:mucin weight ratio 1:1.13. (C) Rheological analysis of a 100 mg/mL T7-MELR solution in ultrapure water at 37°C for different times. The elastic modulus (G') is plotted in black and the storage modulus (G'') in red.

Soft hydrogels favor the interaction with (bio)surfaces as they are easily deformable, thereby adapting to the surface's topography and increasing the contact area [60]. Thus, these mechanical properties are beneficial for the intended use of the T7-MELR.

4.4. T7-MELR mucin interaction

4.4.1. Turbidimetry

Turbidity measurements provide a fast and simple measurement of the interactions between mucoadhesive materials and mucin, as interactions between the material and mucin lead to differently sized aggregates at different material proportions, thus affecting the absorbance of the resulting suspension [61]. As seen in Figure 4A, mucin exhibits an absorbance of 0.08 (a.u.). Increasing the concentration of T7-MELR has a negligible effect until 0.5 mg/mL, concentration

from which the turbidity rapidly increases with increasing amounts of T7-MELR, reaching a maximum at 0.75 mg/mL, to rapidly decrease again at higher concentrations. This behavior has been observed previously for other mucoadhesive polymers [57, 62, 63]. Changes in solution turbidity occur due to the formation of different mucin-particle aggregates in the presence of different amounts of T7-MELR. As a control, turbidity measurements were performed with increasing T7-MELR concentrations (Figure 4A, in red). As can be seen, an increase in T7-MELR concentration has a minor effect on turbidity, thus meaning that the turbidity profile observed in the T7-MELR-mucin mixtures is directly related to the interaction between them, exhibiting different turbidity values as result of the differences in aggregate size. SEM images (see Supporting Information) show that the macroscopic structures formed when T7-MELR and mucin are mixed are different to those obtained with each component separately, thus indicating that the materials interact.

4.4.2. Size and Z-Potential

4.4.2.1. Particle size

The mean particle size of mucin and mixtures thereof with increasing amounts of T7-MELR were measured (Figure 4C). Mucin particles have a relatively small diameter as aggregates were precipitated during sample preparation. Mucin particle suspension exhibits an average particle size of about 280 nm, with a polydispersity index (PdI) of 0.25 (Figure 4D).

Concentrations below 0.613 mg/mL have little effect on particle size and PdI. Above this concentration, the size and PdI start to increase rapidly up to a maximum at 0.75 mg/mL of T7-MELR. Higher concentrations result in an opposite effect, with Z-size and PdI decreasing to a minimum at 1 mg/mL T7-MELR. Further increases in the T7-MELR concentration stabilize the size at around 200 nm but increase PdI up to 0.4.

4.4.2.2. Z-Potential

Charge interactions play a key role as they are one of the first interactions to arise once the materials come into contact and serve to stabilize the system. The Z-potential of mucin particle suspensions containing increasing amounts of mucoadhesive serves to characterize the surface

charge exchange between the components. The Z-potential of the pure mucin suspension was found to be -23.6 mV (Figure 4B), in good accordance with values found in literature [54, 64, 65]. Increasing the amount of T7-MELR increases this negative Z-potential, reaching positive values at 0.75 mg/mL, which suggests that, above this concentration, mucin particles start to be completely covered by the T7-MELR.

The previously observed turbidity and size profile (Figure 4A and C) can be explained in terms of aggregation/non-aggregation of the mucin particles as result of electrostatic interactions, as seen by Z-potential measurements. At concentrations below 0.65 mg/mL mucoadhesive binds to mucin particles, increasing Z-potential but not turbidity nor mean particle size; above this concentrations, there is enough T7-MELR to start bridging mucin particles, further increasing Z-potential and highly increasing turbidity and mean particle size. It appears that mucin particles are bridged rather than being completely covered as the Z-potential remains negative. The positive charge mucin particles exhibit at 0.75 mg/mL and above (Figure 4B) hinders them to aggregate, lowering suspensions turbidity and mean particle size.

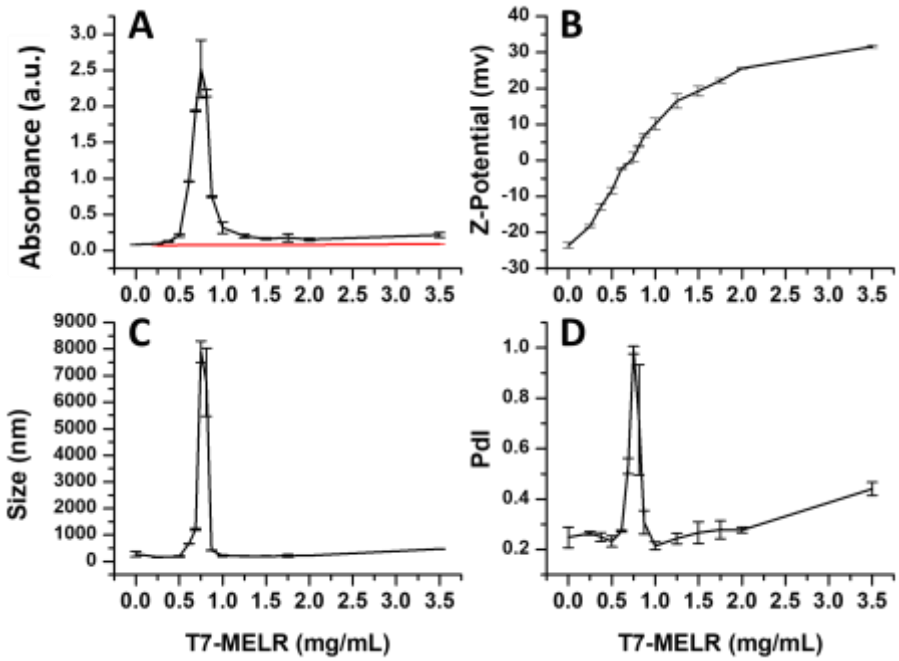

Figure 4. (A) Turbidity profiles for solutions of increasing T7-MELR concentration (red line) and the same solutions in the presence of 0.85 mg/mL mucin suspension (black) at 650 nm. (B) Z-Potential measurements of a 0.85 mg/mL suspension of mucin with increasing amounts of T7-MELR. (C) The graph shows the variation in the size (nm) of the mucin particle suspension with increasing amounts of T7-MELR. (D) Variation in the polydispersity index (PdI) of the mucin suspension with increasing amounts of T7-MELR.

The good concordance in terms of the concentration at which trends for the different measurements (turbidity, size and Z-potential) change is worth mentioning. For turbidity and particle-size measurements, the aggregates start to decrease in size above 0.75 mg/mL (i.e. at a 1:1.13 T7-MELR to mucin proportion), which is the concentration at which mucin particles' Z-potential changes from negative to positive (Figure 4B). The 1:1.13 T7-MELR to mucin proportion was considered as the ratio at which interactions maximize. Next step was to test the effect of mucin, at this proportion, over the previously measured properties of the T7-MELR.

4.4.3. Differential scanning calorimetry (DSC)

The thermal properties of the T7-MELR-mucin mixture, in a 1:1.13 T7-MELR to mucin ratio were measured by DSC (Figure 2) and the T_t and latent heat of transition compared to those for the individual components (100 mg/mL for the MELR and 113 mg/mL for mucin). The T_t of the mixture was found to be 17.79°C, with a latent heat of transition of -5.26 $J \cdot g^{-1}$, very similar to that of the T7-MELR at 100 mg/mL. A 113 mg/mL mucin solution in ultrapure water shows no observable thermal transitions in the temperature range studied (Figure 2). Thus, the transition observed for the T7-MELR mixture with mucin is exclusively due to the ELR. The reduction in T_t for the mixture might be due to a "salting out" effect of the mucin over the T7-MELR. Mucins are large molecules with great affinity towards water molecules, which compete with the T7-MELR for its hydration, thus, disrupting the water clathrates that hydrate the recombinamer. Interestingly, although the transition of the mixture is less pronounced than that of the T7-MELR alone, it extends over a wider range of temperatures, reaching virtually the same latent heat of fusion.

4.4.4. Rheological measurements: mechanical properties

Figure 3B shows the evolution of the elastic modulus (G') and the storage modulus (G'') for the T7-MELR-mucin mixture, at a proportion T7-MELR to mucin of 1:1.13. As can be seen, the system is, once again, temperature-responsive (G' and G'' are temperature-dependent) and the system is able to form soft hydrogels, as can be seen from the crossover of G' with G'', although this occurs at different temperatures and with different values when compared with the T7-MELR

alone. For the T7-MELR, the crossover takes place at 28.0°C and at 101 Pa while for the T7-MELR-mucin mixture it takes place at 21.2°C and 147 Pa. Such results confirm the salting-out effect of the mucin observed by DSC (Figure 2) and that the interaction with mucin does not hinder the thermogelling properties of the T7-MELR. These findings are consistent with the block-design of the T7-MELR, where each property is codified in different blocks, whose properties coexist but do not interfere with each other.

4.4.5. Tensile measurements

Although the previous characterization techniques provide evidence regarding the mucin-interacting capacity of the T7-MELR designed herein, they do not offer a quantifiable value of the strength of this interaction. In order to quantify the adhesion properties of the designed T7-MELR, tensile measurements were performed, quantifying both the maximum detachment force (MDF) and the work of adhesion (WA). To determine the MDF and WA of the T7-MELR-mucin system, three different control of experiments (ELR-ELR, ELR-FILTER and MUCIN-MUCIN) were analyzed in order to exclude artifacts resulting from the breakage cohesive forces of any of the components.

As seen in Figure 5, the MDF and WA for ELR-ELRs show the highest values, thus indicating the strong internal cohesive forces of the T7-MELR hydrogel. For the MUCIN-MUCIN the MDF values were also higher than for the ELR-MUCIN system, thus indicating, as in the case of the ELR-ELR, that mucin is sufficiently cohesive to not interfere in the measurements. T7-MELR was also tested against plain filter paper (ELR-FILTER). The low MDF and WA values for ELR-FILTER indicate that the T7-MELR does not interact strongly with the underlying surface when brought into contact. Finally, we measured the MDF and WA for the ELR-MUCIN system. As can be seen from the figure, the MDF for the ELR-MUCIN system is lower than those for ELR-ELR and MUCIN-MUCIN, thus indicating that the system detaches at the interface of the T7-MELR and mucin. It is also noticeable that the MDF and the WA for the ELR-MUCIN system are much higher than the MDF for ELR-FILTER, thus indicating the specificity of the interaction towards mucin. The WA for ELR-MUCIN was found to be 600 μJ, a higher value than those

found in the literature for other mucoadhesives [66], although comparison of results should be done carefully, as the experimental setup greatly influences results [67].

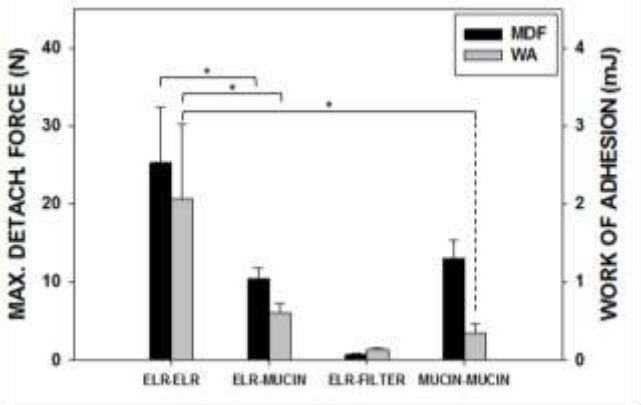

Figure 5. Maximum detachment force and work of adhesion for different test conditions.

4.5. Caco-2 binding and competition assay

4.5.1. Caco-2 binding assays

Is essential that any material intended to be in contact with a biological tissue is neither cytotoxic nor affects cell behavior. Along the different time-points tested, Alamar-Blue reduction levels demonstrated the normal metabolic activity of Caco-2 cells treated with different concentrations of both ELRs, finding no statistical differences with untreated cells. Being assessed the non-cytotoxic effects of both, the MELR and the T7-MELR (see Supporting Information), next step was to assess its cell binding properties. Our design included a TfR-binding sequence that might increase the amount of bounded MELR given its ability to interact with the layer of epithelial cells beneath the mucus. Quantification of the attached MELRs was done via chemical modification with FITC (See Supporting Information).

As shown in Figure 6A, the amount of MELR adhered to the Caco-2 monolayer varies with time and concentration. In one hand, at the lowest concentration tested (1 mg/mL), the amount of material adhered after incubation for 120 minutes increases by a factor of 1.5 for the MELR and by a factor of 1.4 for the T7-MELR with respect to the amount adhered at 30 minutes. At 5 mg/mL, the amount of attached mucoadhesive increases by a factor of 1.6 for the MELR and 1.7 for the T7-MELR. In the other hand, for the shortest time tested (30 minutes), the amount of MELR

attached to the Caco-2 monolayer after exposure to the 5 mg/mL solution is 2.3-fold greater than for the 1 mg/mL solution, with this value increasing to 3.3 for the T7-MELR. Upon exposure for 120 minutes, this factor increases by 2.5-fold for the MELR and 4-fold for the T7-MELR. Thus, FITC fluorescence showed a clear time- and concentration-dependence for both MELRs, with more MELR being attached at higher concentration and the longer the exposure.

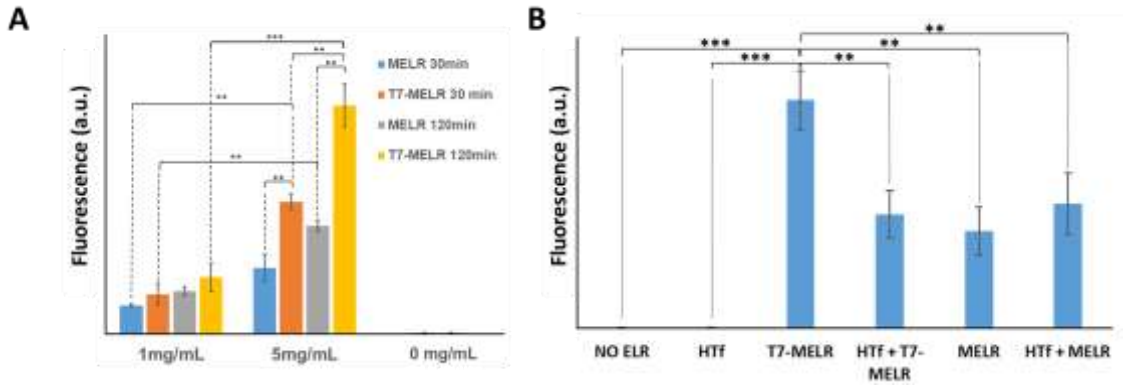

Figure 6. (A) FITC fluorescence intensities measured in the cell-binding assays. Cells were co-incubated for 30 minutes and 120 minutes. The fluorescence measured for untreated cells was used as negative control. (B) Competition assay with T7-MELR and HTf. When needed, cells were incubated for 120 min with a 2 mg/mL HTf solution in complete media. After HTf treatment, incubation with ELRs and ELRs+HTf was carried out for 120 minutes at 5 mg/mL (43 µM) for ELRs and 2 mg/mL (25 µM) for HTf, dissolved in complete medium.

In addition to the concentration- and time-dependence, results show that more MELR is retained when the T7 amino-acid sequence is present. This increase is also time- and concentration-dependent, as can be seen in Figure 6A. For a concentration of 1 mg/mL, there is no significant difference between the MELRs with and without T7 at any incubation time, whereas at a concentration of 5 mg/mL there is a marked increase in the amount of MELR retained. Upon incubation for 30 minutes, the presence of the T7 amino-acid sequence increases the amount of MELR retained twofold, with this value increasing to 2.1-fold after 120 minutes.

4.5.2. Caco-2 competitive binding assays

The previous results suggested an active role of the T7 sequence in increasing the amount of T7-MELR that remains attached to the Caco-2 monolayer. In order to confirm such result, we performed a competition assay with HTf, which has a marked affinity for TfR. As such, we used a HTf concentration of 2 mg/mL (25 µM), much higher than its Kd (10^{-7}-10^{-9}M) [68, 69], to ensure that all TfRs are saturated with HTf.

It can be seen from Figure 6B the amount of T7-MELR retained decreases drastically in the presence of HTf, reaching values of the order of those obtained for MELR, whereas the presence of HTf did not influence the amount of MELR bounded to the Caco-2 monolayer. These results indicate, first, the active role of the T7 sequence in increasing the amount of MELR attached to the Caco-2 monolayer, which is a well-accepted model of the enterocytes underlying the mucus [70], and second, the non-interference between the mucus interacting tail and HTf. Fluorescence microscopy images (SFigure16) show the same results in a qualitative manner. Thus, the amount of FITC fluorescence is similar in those cells treated with MELR and those treated first with HTf (SFigure16, A-B), whereas it is markedly increased when cells are treated with the T7-MELR (SFigure16, C-D).

4.6. *In vivo* assay

Confirmed *in vitro* the mucoadhesive properties of T7-MELR, *in vivo* experiments were performed. *In vivo* experiments are essential, as there is no *in vitro* model capable of mimicking the complexity of a living being. The use of fed rats is not casual given the more realistic situation it represents, especially considering the fact that fasting conditions might lead to an overestimation of the mucoadhesive properties, as the flushing and dilution effect exerted by food and water is not taken into consideration. Secondly, the fact that it takes about 8 to 12 hours [71] (or even longer [72]) to completely empty the GIT, which may be detrimental to animal welfare. Finally, GIT mobility is affected in fasting animals [73].

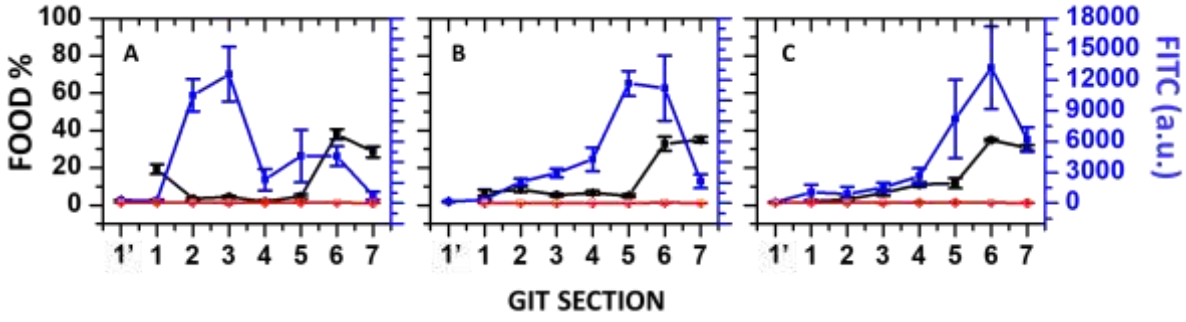

Figure 7. Food (black line) and FITC (blue line) transit profile at (A) 3, (B) 5 and (C) 7 hours post administration of the T7-MELR, along the different GIT sections (sections 1 to 7). 1' stands for stomach food content. Red line stands for the fluorescence found in the control rats.

Taking advantage of the thermoresponsiviness of the T7-MELR it was gavage in liquid state (at 4 ºC), and let to jellify in the stomach of the rat as it is heated above its T_t. As can be seen in Figure 7, T7-MELR transit exhibits a different profile to that for food. Differences may arise because of several factors. The initial burst release from the stomach throughout the gastrointestinal tract appears to be due to the flushing and dilution effect of water ingested after the administration of T7-MELR as it is ahead of the food. Interestingly, once food has been emptied from the different GIT sections, a marked amount of T7-MELR is still found. This finding suggests that, although diluted by water uptake, T7-MELR is able to withstand the flushing effect of food and remains attached to the GIT walls.

5. Conclusions

Current strategies for improving mucosal drug delivery focus on mucoadhesion and on interacting with the underlying epithelial cells by way of specific receptor binding sequences, which extend the residence time while keeping the drug-delivery material in close contact with the absorbing surface.

In this work, we have designed, bioproduced, purified and characterized two thermoresponsive hydrogel-forming ELRs with mucoadhesive properties. Rheological measurements showed that a soft hydrogel, which is beneficial for interaction with the mucus, is eventually formed [74, 75]. Mucoadhesive properties have been studied from the point of view of different mucoadhesion theories using a variety of techniques that corroborate our working hypothesis, namely that the addition of a high molecular weight, hydrophilic and positively charged tail to a thermogelling structure allows the ELR to efficiently interact with the mucus. Moreover, we have produced an improved version that is able to interact with the gastrointestinal epithelium underlying the mucus, thereby combining the advantages of both types of interactions in a single molecule.

With regard to our results, inclusion of the TfR-binding motif (T7 sequence) in the MELR molecule has improved, up to four fold, the ability of the designed MELR to interact with the epithelial cells underlying the mucus in a Caco-2 cell model without negatively affecting its biocompatibility. This cell-material interaction serves as a mechanism to increase the amount of

material that remains attached to the epithelial monolayer, thereby prolonging the residence time and increasing the amount of drug exposed to the mucosa. Mucoadhesive properties were further corroborated in an *in vivo* rat model in which the transit of the T7-MELR was compared with that of food. The slower transit of the mucoadhesive compared with food was associated with its mucoadhesive properties.

The amino-acid composition of these MELRs is resistant to unspecific proteolysis [76] and, also, the T7-MELR presented in this manuscript if forming an hydrogel under the tested conditions, which further difficult its degradation [77], extending its residence time. Nevertheless, with time, as a proteinaceous material it is, it would end up being totally degraded in the gastrointestinal tract, whereas its amino-acid composition ensures non-toxic degradation products. Due to the delayed degradation of the T7-MELR, as well as for the rapid turnover rate of the TfR of few minutes, we do expect the T7-MELR to be internalized carrying the drug prior to its degradation. The study of the uptake of a model drug carried by the T7-MELR is beyond the scope of this manuscript, focused in the demonstration of the mucoadhesive and cell-binding properties of the T7-MELR.

In conclusion, with this work, we have set the molecular basis and interactions necessary for an ELR to adhere via multiple processes to *mucosae*, a tissue widely found in human body, extending its residence time and thus the time of exposure to the delivered drug. The mucoadhesive and cell-binding properties, together with the intrinsic properties of ELRs (i.e. being thermoresponsive and solft-gel forming), integrated in a single molecule, make this material a good candidate for interacting with mucosa. Future work will focus in the delivery of a model drug into the GIT as well as the search of the application of these materials to other *mucosae*, such as eyes or the respiratory mucosa, searching to develop improved drug delivery systems.

6. Acknowledgments

The authors are grateful for funding from the European Commission (NMP-2014-646075), the Spanish Government (PCIN-2015-010, MAT2015-68901-R, MAT2016-78903-R, MAT2016-79435-R), Junta de Castilla y León (VA015U16) and Centro en Red de Medicina Regenerativa y Terapia Celular de Castilla y León.

7. References

[1] Scrivener. D.D.S CA, Schantz CW. Penicillin: New Methods for its Use in Dentistry. The Journal of the American Dental Association 1947;35:644-7.
[2] Fuhrmann G, Grotzky A, Lukić R, Matoori S, Luciani P, Yu H, Zhang B, Walde P, Schlüter AD, Gauthier MA, Leroux J-C. Sustained gastrointestinal activity of dendronized polymer–enzyme conjugates. Nature Chemistry 2013;5:582-9.
[3] Tibbitt MW, Dahlman JE, Langer R. Emerging Frontiers in Drug Delivery. Journal of the American Chemical Society 2016;138:704-17.
[4] Sau-Hung Spence L, Robinson JR. The contribution of anionic polymer structural features to mucoadhesion. Journal of Controlled Release 1987;5:223-31.
[5] Smart JD. The basics and underlying mechanisms of mucoadhesion. Advanced Drug Delivery Reviews 2005;57:1556-68.
[6] Turner JR. Intestinal mucosal barrier function in health and disease. Nat Rev Immunol 2009;9:799-809.
[7] Johansson MEV, Sjövall H, Hansson GC. The gastrointestinal mucus system in health and disease. Nature reviews Gastroenterology & hepatology 2013;10:352-61.
[8] Bansil R, Turner BS. Mucin structure, aggregation, physiological functions and biomedical applications. Current Opinion in Colloid & Interface Science 2006;11:164-70.
[9] Yu T, Andrews PG, Jones SD. Mucoadhesion and Characterization of Mucoadhesive Properties. In: das Neves J, Sarmento B, editors. Mucosal Delivery of Biopharmaceuticals: Biology, Challenges and Strategies. Boston, MA: Springer US; 2014. p. 35-58.
[10] Woertz C, Preis M, Breitkreutz J, Kleinebudde P. Assessment of test methods evaluating mucoadhesive polymers and dosage forms: An overview. European Journal of Pharmaceutics and Biopharmaceutics 2013;85:843-53.
[11] Singh I, Rana V. Techniques for the Assessment of Mucoadhesion in Drug Delivery Systems: An Overview. Journal of Adhesion Science and Technology 2012;26:2251-67.
[12] Shin M, Kim K, Shim W, Yang JW, Lee H. Tannic Acid as a Degradable Mucoadhesive Compound. ACS Biomaterials Science & Engineering 2016;2:687-96.
[13] Oh S, Borrós S. Mucoadhesion vs mucus permeability of thiolated chitosan polymers and their resulting nanoparticles using a quartz crystal microbalance with dissipation (QCM-D). Colloids and Surfaces B: Biointerfaces 2016;147:434-41.
[14] Mazoniene E, Joceviciute S, Kazlauske J, Niemeyer B, Liesiene J. Interaction of cellulose-based cationic polyelectrolytes with mucin. Colloids and Surfaces B: Biointerfaces 2011;83:160-4.
[15] Hägerström H, Edsman K. Interpretation of mucoadhesive properties of polymer gel preparations using a tensile strength method. Journal of Pharmacy and Pharmacology 2001;53:1589-99.
[16] Bernkop-Schnürch A, Guggi D, Pinter Y. Thiolated chitosans: development and in vitro evaluation of a mucoadhesive, permeation enhancing oral drug delivery system. Journal of Controlled Release 2004;94:177-86.
[17] Bernkop-Schnurch A, Schwarz V, Steininger S. Polymers with thiol groups: a new generation of mucoadhesive polymers? Pharmaceutical research 1999;16:876-81.
[18] Irache JM, Durrer C, Duchêne D, Ponchel G. In vitro study of lectin-latex conjugates for specific bioadhesion. Journal of Controlled Release 1994;31:181-8.
[19] Cartiera MS, Johnson KM, Rajendran V, Caplan MJ, Saltzman WM. The uptake and intracellular fate of PLGA nanoparticles in epithelial cells. Biomaterials 2009;30:2790-8.
[20] Dyawanapelly S, Koli U, Dharamdasani V, Jain R, Dandekar P. Improved mucoadhesion and cell uptake of chitosan and chitosan oligosaccharide surface-modified polymer nanoparticles for mucosal delivery of proteins. Drug delivery and translational research 2016;6:365-79.

[21] Laffleur F, Bernkop-Schnurch A. Strategies for improving mucosal drug delivery. Nanomedicine (London, England) 2013;8:2061-75.
[22] Montisci M-J, Dembri A, Giovannuci G, Chacun H, Duchêne D, Ponchel G. Gastrointestinal Transit and Mucoadhesion of Colloidal Suspensions of Lycopersicon Esculentum L. and Lotus Tetragonolobus Lectin-PLA Microsphere Conjugates in Rats. Pharmaceutical research 2001;18:829-37.
[23] Clark MA, Hirst BH, Jepson MA. Lectin-mediated mucosal delivery of drugs and microparticles. Adv Drug Deliv Rev 2000;43:207-23.
[24] Ponchel G, Irache J-M. Specific and non-specific bioadhesive particulate systems for oral delivery to the gastrointestinal tract. Advanced Drug Delivery Reviews 1998;34:191-219.
[25] Chen M-L. Lipid excipients and delivery systems for pharmaceutical development: A regulatory perspective. Advanced Drug Delivery Reviews 2008;60:768-77.
[26] Morgan EH. Transferrin, biochemistry, physiology and clinical significance. Molecular Aspects of Medicine 1981;4:1-123.
[27] Tirosh B, Khatib N, Barenholz Y, Nissan A, Rubinstein A. Transferrin as a Luminal Target for Negatively Charged Liposomes in the Inflamed Colonic Mucosa. Molecular Pharmaceutics 2009;6:1083-91.
[28] Kolachala VL, Sesikeran B, Nair KM. Evidence for a sequential transfer of iron amongst ferritin, transferrin and transferrin receptor during duodenal absorption of iron in rat and human. World journal of gastroenterology 2007;13:1042-52.
[29] Amet N, Wang W, Shen WC. Human growth hormone-transferrin fusion protein for oral delivery in hypophysectomized rats. Journal of controlled release : official journal of the Controlled Release Society 2010;141:177-82.
[30] Hamid Akash MS, Rehman K, Chen S. Natural and Synthetic Polymers as Drug Carriers for Delivery of Therapeutic Proteins. Polymer Reviews 2015;55:371-406.
[31] Wang Z, Zhao Y, Jiang Y, Lv W, Wu L, Wang B, Lv L, Xu Q, Xin H. Enhanced anti-ischemic stroke of ZL006 by T7-conjugated PEGylated liposomes drug delivery system. Scientific Reports 2015;5:12651.
[32] Han L, Huang R, Liu S, Huang S, Jiang C. Peptide-Conjugated PAMAM for Targeted Doxorubicin Delivery to Transferrin Receptor Overexpressed Tumors. Molecular Pharmaceutics 2010;7:2156-65.
[33] Du W, Fan Y, Zheng N, He B, Yuan L, Zhang H, Wang X, Wang J, Zhang X, Zhang Q. Transferrin receptor specific nanocarriers conjugated with functional 7peptide for oral drug delivery. Biomaterials 2013;34:794-806.
[34] Lee JH, Engler JA, Collawn JF, Moore BA. Receptor mediated uptake of peptides that bind the human transferrin receptor. European Journal of Biochemistry 2001;268:2004-12.
[35] Simon-Assmann P, Turck N, Sidhoum-Jenny M, Gradwohl G, Kedinger M. In vitro models of intestinal epithelial cell differentiation. Cell Biology and Toxicology 2007;23:241-56.
[36] Hubatsch I, Ragnarsson EGE, Artursson P. Determination of drug permeability and prediction of drug absorption in Caco-2 monolayers. Nat Protocols 2007;2:2111-9.
[37] Widera A, Norouziyan F, Shen WC. Mechanisms of TfR-mediated transcytosis and sorting in epithelial cells and applications toward drug delivery. Advanced Drug Delivery Reviews 2003;55:1439-66.
[38] Lim C-J, Norouziyan F, Shen W-C. Accumulation of transferrin in Caco-2 cells: A possible mechanism of intestinal transferrin absorption. Journal of Controlled Release 2007;122:393-8.
[39] Mudie DM, Amidon GL, Amidon GE. Physiological Parameters for Oral Delivery and in Vitro Testing. Molecular Pharmaceutics 2010;7:1388-405.
[40] McConnell EL, Fadda HM, Basit AW. Gut instincts: explorations in intestinal physiology and drug delivery. Int J Pharm 2008;364:213-26.
[41] Rodríguez-Cabello JC, Martín L, Alonso M, Arias FJ, Testera AM. “Recombinamers” as advanced materials for the post-oil age. Polymer 2009;50:5159-69.

[42] Rodríguez-Cabello JC, Arias FJ, Rodrigo MA, Girotti A. Elastin-like polypeptides in drug delivery. Advanced Drug Delivery Reviews 2016;97:85-100.
[43] Hidalgo IJ. Cultured Intestinal Epithelial Cell Models. In: Borchardt RT, Smith PL, Wilson G, editors. Models for Assessing Drug Absorption and Metabolism. Boston, MA: Springer US; 1996. p. 35-50.
[44] Rodríguez-Cabello JC, Girotti A, Ribeiro A, Arias FJ. Synthesis of Genetically Engineered Protein Polymers (Recombinamers) as an Example of Advanced Self-Assembled Smart Materials. In: Navarro M, Planell JA, editors. Nanotechnology in Regenerative Medicine: Methods and Protocols. Totowa, NJ: Humana Press; 2012. p. 17-38.
[45] Rossi S, Ferrari F, Bonferoni MC, Caramella C. Characterization of chitosan hydrochloride–mucin interaction by means of viscosimetric and turbidimetric measurements. European Journal of Pharmaceutical Sciences 2000;10:251-7.
[46] Ivarsson D, Wahlgren M. Comparison of in vitro methods of measuring mucoadhesion: Ellipsometry, tensile strength and rheological measurements. Colloids and Surfaces B: Biointerfaces 2012;92:353-9.
[47] Hagesaether E, Sande SA. In vitro measurements of mucoadhesive properties of six types of pectin. Drug development and industrial pharmacy 2007;33:417-25.
[48] Tavelin S, Gråsjö J, Taipalensuu J, Ocklind G, Artursson P. Applications of Epithelial Cell Culture in Studies of Drug Transport. In: Wise C, editor. Epithelial Cell Culture Protocols. Totowa, NJ: Humana Press; 2002. p. 233-72.
[49] Martin L, Arias FJ, Alonso M, Garcia-Arevalo C, Rodriguez-Cabello JC. Rapid micropatterning by temperature-triggered reversible gelation of a recombinant smart elastin-like tetrablock-copolymer. Soft Matter 2010;6:1121-4.
[50] Fernández-Colino A, Arias FJ, Alonso M, Rodríguez-Cabello JC. Self-Organized ECM-Mimetic Model Based on an Amphiphilic Multiblock Silk-Elastin-Like Corecombinamer with a Concomitant Dual Physical Gelation Process. Biomacromolecules 2014;15:3781-93.
[51] Urry DW. What Sustains Life? Consilient Mechanisms for Protein-Based Machines and Materials: Birkhäuser Basel; 2006.
[52] Piña MJ, Girotti A, Santos M, Rodríguez-Cabello JC, Arias FJ. Biocompatible ELR-Based Polyplexes Coated with MUC1 Specific Aptamers and Targeted for Breast Cancer Gene Therapy. Molecular Pharmaceutics 2016;13:795-808.
[53] Girotti A, Orbanic D, Ibáñez-Fonseca A, Gonzalez-Obeso C, Rodríguez-Cabello JC. Recombinant Technology in the Development of Materials and Systems for Soft-Tissue Repair. Advanced Healthcare Materials 2015;4:2423-55.
[54] Khutoryanskiy VV. Advances in Mucoadhesion and Mucoadhesive Polymers. Macromolecular Bioscience 2011;11:748-64.
[55] Hubbell JA, Thomas SN, Swartz MA. Materials engineering for immunomodulation. Nature 2009;462:449-60.
[56] Sriamornsak P, Wattanakorn N, Nunthanid J, Puttipipatkhachorn S. Mucoadhesion of pectin as evidence by wettability and chain interpenetration. Carbohydrate Polymers 2008;74:458-67.
[57] Fefelova NA, Nurkeeva ZS, Mun GA, Khutoryanskiy VV. Mucoadhesive interactions of amphiphilic cationic copolymers based on [2-(methacryloyloxy)ethyl]trimethylammonium chloride. International Journal of Pharmaceutics 2007;339:25-32.
[58] Rodrıguez-Cabello JC, Reguera J, Alonso M, Parker TM, McPherson DT, Urry DW. Endothermic and exothermic components of an inverse temperature transition for hydrophobic association by TMDSC. Chemical Physics Letters 2004;388:127-31.
[59] Fernández-Colino A, Arias FJ, Alonso M, Rodríguez-Cabello JC. Amphiphilic Elastin-Like Block Co-Recombinamers Containing Leucine Zippers: Cooperative Interplay between Both Domains Results in Injectable and Stable Hydrogels. Biomacromolecules 2015;16:3389-98.
[60] Anne M. Grillet NBWaLMG. Polymer Gel Rheology and Adhesion. In: Vicente Jd, editor. Rheology: Intech; 2012. p. 350.

[61] Dubolazov AV, Nurkeeva ZS, Mun GA, Khutoryanskiy VV. Design of mucoadhesive polymeric films based on blends of poly(acrylic acid) and (hydroxypropyl)cellulose. Biomacromolecules 2006;7:1637-43.
[62] Sogias IA, Williams AC, Khutoryanskiy VV. Why is Chitosan Mucoadhesive? Biomacromolecules 2008;9:1837-42.
[63] Maleki A, Lafitte G, Kjøniksen A-L, Thuresson K, Nyström B. Effect of pH on the association behavior in aqueous solutions of pig gastric mucin. Carbohydrate Research 2008;343:328-40.
[64] Takeuchi H, Thongborisute J, Matsui Y, Sugihara H, Yamamoto H, Kawashima Y. Novel mucoadhesion tests for polymers and polymer-coated particles to design optimal mucoadhesive drug delivery systems. Advanced Drug Delivery Reviews 2005;57:1583-94.
[65] Sriamornsak P, Wattanakorn N, Takeuchi H. Study on the mucoadhesion mechanism of pectin by atomic force microscopy and mucin-particle method. Carbohydrate Polymers 2010;79:54-9.
[66] Grabovac V, Guggi D, Bernkop-Schnürch A. Comparison of the mucoadhesive properties of various polymers. Advanced Drug Delivery Reviews 2005;57:1713-23.
[67] Eshel-Green T, Bianco-Peled H. Mucoadhesive acrylated block copolymers micelles for the delivery of hydrophobic drugs. Colloids and surfaces B, Biointerfaces 2016;139:42-51.
[68] Fuchs H, Gessner R. Iodination significantly influences the binding of human transferrin to the transferrin receptor. Biochimica et biophysica acta 2002;1570:19-26.
[69] Dautry-Varsat A, Ciechanover A, Lodish HF. pH and the recycling of transferrin during receptor-mediated endocytosis. Proceedings of the National Academy of Sciences 1983;80:2258-62.
[70] Natoli M, Leoni BD, D'Agnano I, Zucco F, Felsani A. Good Caco-2 cell culture practices. Toxicology in Vitro 2012;26:1243-6.
[71] Albrecht K, Greindl M, Kremser C, Wolf C, Debbage P, Bernkop-Schnürch A. Comparative in vivo mucoadhesion studies of thiomer formulations using magnetic resonance imaging and fluorescence detection. Journal of controlled release : official journal of the Controlled Release Society 2006;115:78-84.
[72] Torjman MC, Joseph JI, Munsick C, Morishita M, Grunwald Z. Effects of Isoflurane on gastrointestinal motility after brief exposure in rats. International Journal of Pharmaceutics 2005;294:65-71.
[73] Mittelstadt SW, Hemenway CL, Spruell RD. Effects of fasting on evaluation of gastrointestinal transit with charcoal meal. Journal of Pharmacological and Toxicological Methods 2005;52:154-8.
[74] Andrews GP, Jones DS. Rheological Characterization of Bioadhesive Binary Polymeric Systems Designed as Platforms for Drug Delivery Implants. Biomacromolecules 2006;7:899-906.
[75] Lenhart JL, Cole PJ. Adhesion Properties of Lightly Crosslinked Solvent-Swollen Polymer Gels. The Journal of Adhesion 2006;82:945-71.
[76] McGowan JWD, Vig PJS, Bidwell GL. The Use of Intransally-delivered Elastin-like Polypeptide for Drug Delivery to the Central Nervous System. The FASEB Journal 2016;30:990.2-.2.
[77] Despanie J, Dhandhukia JP, Hamm-Alvarez SF, MacKay JA. Elastin-like polypeptides: Therapeutic applications for an emerging class of nanomedicines. Journal of controlled release : official journal of the Controlled Release Society 2016;240:93-108.